EFFECT OF SHIP SIDE WAVE UPON THE RESPONSE OF HULL SPRINGING

KUMAI, Toyoji
Research Institute for Applied Mechanics, Kyushu University : Professor

https://doi.org/10.5109/7172624

出版情報：Reports of Research Institute for Applied Mechanics. 20 (66), pp.1-20, 1973. 九州大学応用力学研究所

Reports of Research Institute for Applied Mechanics
Vol. XX, No. 66, 1973

EFFECT OF SHIP SIDE WAVE UPON THE RESPONSE OF HULL SPRINGING

By Toyoji KUMAI*

The paper shows envelopes of ship side wave height measured by self-propelled model of a tanker which is going in regular wave, and the wave-induced vibratory force and response are estimated by using the measured ship side wave with three types of wave pattern in parameter. As a result, it seems that the progressive force exciting hull vibration is distributed along ship length, however the distribted force is almost concentrated in the range of entrance of the hull of a tanker due to the effect of ship side wave distortion.

1. Introduction

As a succeeding part of the author's previous work[1], he investigated the effect of distortion of wave at ship side upon the wave excitation and response of the hull springing based on the measured results of the envelope of the ship side wave height of a self-propelled model tanker in a regular wave. The deformation of the water line of the model which is going in smooth wate is pursued at first and then the envelopes of the relative ship side wave height along ship length are measured for various ratios of wave length to ship length. The measured envelopes of the wave height along ship length are greatly different from those of the sea wave profile, as assumed in the author's previous calculation. The paper gives some results of model experiments and calculations of the wave exciting force including buoyant force and the rsesponse of the springing of a tanker, where the measured results of the relative ship side wave height are used.

2. Envelope of Ship Side Wave Height

The shape of envelope of the ship side wave height when a speciall type ship going sea way has been mathematically obtained by Grim[2]. The results of his investigation is of interest where he asserts that the shape of the envelope of the ship side wave is changing periodically along ship length and the less wave height gets the nearer to the ship stern. Sinec the pattern of the envelope of ship side wave height depends on ship form, the theoretical results of envelope

* Professor, Research Institute for Applied Mechanics, Kyushu University, Fukuoka, Japan.

obtained by Grim is not applicable to the present problem. The envelopes of the ship side wave are however obtained from the experiments made on a self-propelled model tanker. The author used an apparatus of electric resistance measurement of draught at stations of a model in the present investigation.

An example of the measured results of the distortion of water line of the model tanker going in smooth water under ballast condition is shown in Fig. 1. It is to be noted that the water line of the ship, when she is going in smooth water is disturbed by bow wave. The sea wave will be superposed on the disturbed water line. What is worth our attention is that the envelope of the relative ship side wave changes periodically, damping itself toward ship stern. The distortion of the wave height measured at ship side in the present experiments is qualitatively similar to the results of mathematical investigation given given by Grim[2], but there is visible increase of the wave height close to the fore perpendicular of the tanker, as seen in Figure 2. Figure 3 shows the

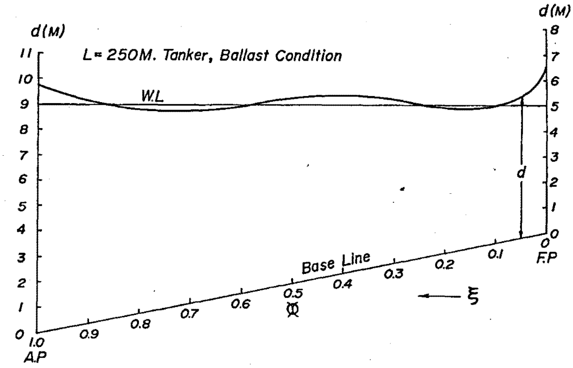

Fig. 1 Deformed water line when model ship is going in smooth water

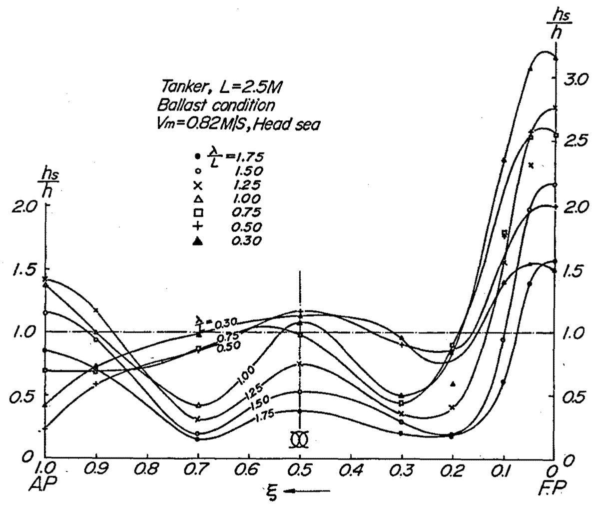

Fig. 2 Envelopes of ship side wave height of self-propelled model of tanker

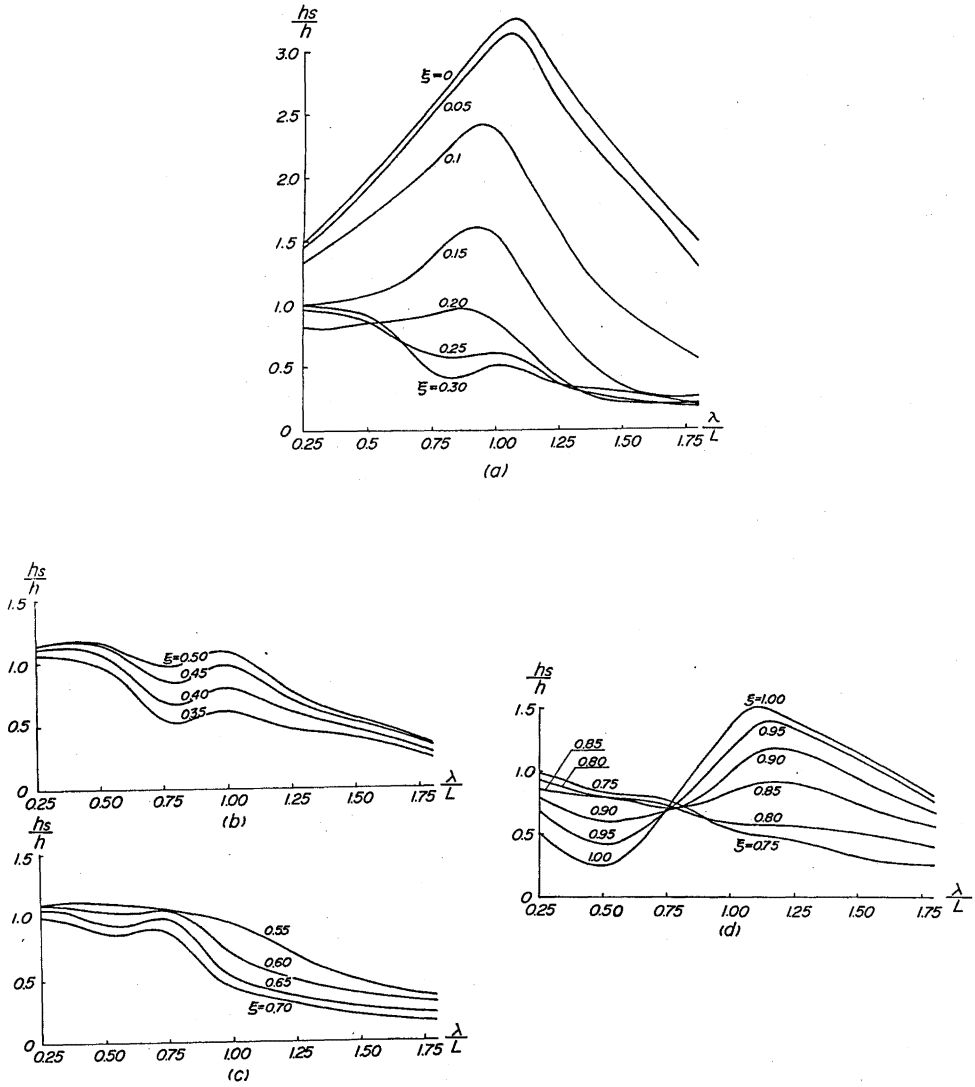

Fig. 3 Ship side wave versus wave length ratio with parameter of ship section

relative wave height versus wave length ratios λ/L with each station in parameter. The maximum relative wave height appears near from $\lambda/L=1.1$, and this wave length is that of the resonance of pitching motion of the ship. It is also noteworthy that measured values of the wave heights close to the stations 3, 7 and 8 are much smaller than those of sea wave.

3. Exciting Force and Response of Springing

Since the cause of occurrence of springing of a ship is considered to be the selective resonance of the ship hull vibration due to periodic wave encounter as shown in model test (see Appendix A1), the exciting force of a spring is assumed to be of the n-th order component of wave force which consist of the virtual added mass force and the buoyant force induced by periodic change of draught of the relative ship side wave height. There n is the ratio of the encounter period to the natural period of two node vertical vibration of a ship hull. The above hull force per unit section is presented by the sum of the time derivative of the momentum of virtual added mass and the buoyant force produced by wave[3], that is,

$$\Delta F = -\frac{\partial}{\partial t}\left(m_e \frac{\partial z}{\partial t}\right) + \Delta F_b \ , \tag{1}$$

where, m_e three-dimensional virtual added mass which periodically change by wave

z draught which varying due to wave

ΔF_b buoyant force

t time co-ordinate

3. 1. Virtual mass force

The three-dimensional virtual added mass of any hull section is written by

$$m_e = JC_V \frac{\rho \pi b_0^2}{2}\left(\frac{b}{b_0}\right)^2 \ . \tag{2}$$

In the above equation, J is defined as local three-dimensional reduction factor of the virtual mass of the hull section and C_V is the two-dimensional coefficient which depends on the form of the cross section of the hull.

The values JC_V of a given section at a given draught is approximately obtained from measurements of the natural frequencies of the two node flexural vibration of the cylindrical model of given hull section with the same length as the ship model, which was measured in air and in water of a given draught[4]. The measured curves of JC_V versus the draught of several hull sections of a tanker model have been already shown in the author's previous paper[1] as examples. For applying the measured results of JC_V of hull sections to the present investigation, the variation of virtual added mass coefficient, that changes due to ship side wave may be approximately expressed by power series of ζ without constant c_0 as follows,

$$\delta JC_V = \sum_{r=1}^{3} c_r \zeta^r \ , \qquad (r=1,\ 2,\ 3) \tag{3}$$

where, $$\zeta=\frac{2z}{h_s}=a_0+\sum_{m=1}^{3}a_m\cos m\left(\omega t-\frac{2\pi L}{\lambda}\xi\right)\ ,\quad (m=1,\ 2,\ 3) \tag{4}$$

h_s	ship side wave height of given section
a_0, a_m	coefficients of cosine series of wave profile
$\xi=\dfrac{x}{L}$	length co-ordinate with origin at fore perpendicular
ω	encounter frequency of ship and wave
c_r	corrected coefficients of power series

In the above equation, c_r $(r=1,\ 2,\ 3)$ are determined from measured results with some correction for each hull section with given draught and given wave height ratio h_s/h. The method of correction for obtaining c_r from measured value of JC_V is shown in Appendix A2. By using the first expression of (4) and substituting (3) into (1), the virtual mass force applied to the given hull section defined in equation (1) is represented as

$$\varDelta F_V=-\frac{\rho\pi b_0{}^2h\omega^2}{4}\left(\frac{b}{b_0}\right)^2\frac{h_s}{h}\cdot\frac{1}{\omega^2}\frac{\partial}{\partial t}\left(\sum_{r=1}^{3}c_r\zeta^r\frac{\partial\zeta}{\partial t}\right)\ . \tag{5}$$

The terms included in the above equation are calculated by using any wave patterns presented by (4) as follows,

$$-\frac{1}{\omega^2}\frac{\partial}{\partial t}\left(\sum_{r=1}^{3}c_r\zeta^r\frac{\partial\zeta}{\partial t}\right)=\sum_{n=1}^{12}C_n\cos(n\omega t-\psi_n)\ , \tag{6}$$

where, $$\psi_n=\frac{2n\pi L}{\lambda}\xi\ ,\qquad (n=1,\ 2,\ \ldots\ldots\ldots\ldots\ 12)$$

The n-th order amplitude and its phase lag are thus obtained from the above equaton. It is to be noted that the amplitude C_n includes coefficients a_0, a_m and c_r are shown in Appendix A2.

3. 2. Buoyant force

The exciting force produced by change of buoyancy due to ship side wave is obtained by similar calculation as that followed in obtaining virtual added mass force. The buoyant force of any hull section is presented by

$$\varDelta F_b=2\rho g\delta A\ , \tag{7}$$

where, δA area of section immersed by wave

The sectional areas of the hull which is changing by immersion and emersion in relation with ship side wave motion, δA, in the above equation is represented by

$$\delta A = b_0 h \frac{c_m(\overline{h}+d)}{h} \frac{\delta A}{c_m(\overline{h}+d)b_0} , \tag{8}$$

where, b_0 half breadth of ship

h height of sea wave

$\overline{h}+d$ maximum draught for calculating the sectional area

c_m midship section coefficient at the draught $\overline{h}+d$

In the above equation, the ratio $\delta A/c_m(\overline{h}+d)b_0$ is calculated with respect to any ship section versus change of draught, and the buoyancy which changes by wave motion is approximately represented by power series with respect to ζ and lastly presented by cosine series, that

$$\frac{\delta A}{c_m(h+d)b_0} = \sum_{r=1}^{3} k_r \zeta^r = \sum_{n=1}^{9} B_n \cos(n\omega t - \psi_n) , \quad (r=1, 2, 3) \tag{9}$$

The buoyant force of the n-th order component is then expressed by

$$\Delta F_{bn} \doteqdot 2\rho g b_0 h \frac{c_m(\overline{h}+d)}{h} B_n \cos(n\omega t - \psi_n) , \tag{10}$$

where, B_n is the n-th order component of cosine series, including a_0, a_m and k_r, as shown in Appendix $A3$.

3. 3. Total exciting force and response

The exciting force of two node vertical vibration of the hull, which vibrates with normal mode η is expressed by the sum of the virtual mass force and buoyant force as follows;

$$F_n = F_{vn} + F_{bn} = \int_0^L \Delta F dx = \frac{\rho \pi b_0^2 h \omega^2 L}{4} \mu_n (\cos n\omega t - \phi_n) , \tag{11}$$

where, $$\mu_n = \sqrt{G_n^2 + H_n^2}$$

$$\left.\begin{aligned} G_n &= \int_0^1 \left\{ \left(\frac{b}{b_0}\right)^2 \frac{h_s}{h} C_n + \frac{8g}{\pi b_0 \omega^2} \frac{c_m(\overline{h}+d)}{h} B_n \right\} \eta \cos\psi_n d\xi , \\ H_n &= \int_0^1 \left\{ \left(\frac{b}{b_0}\right)^2 \frac{h_s}{h} C_n + \frac{8g}{\pi b_0 \omega^2} \frac{c_m(\overline{h}+d)}{h} B_n \right\} \eta \sin\psi_n d\xi , \end{aligned}\right\} \tag{12}$$

$$\phi_n = \tan^{-1}\left(\frac{H}{G}\right)_n$$

$$\psi_n = \frac{2n\pi L}{\lambda} \xi$$

L ship length

n the ratio of encounter period of ship and wave to the period of natural frequency of the ship hull

With regards to integral of equation (12), if we replace the force envelope some integrable function as an approach, the analytical integral will be carried out provided that the maximum value of the envelope in each n-value between $\xi=0$ to $\xi=1/4$ is given. An example of the analytical integral of the progressive force as an approach is shown in Appendix A4.

The acceleration response at the bow of the ship is presented by

$$a=\frac{cg\pi F_n}{\Delta_1\delta}\ , \qquad (13)$$

where,
- a acceleration at the fore perpendicular
- F_n exciting force applied at the fore perpendicular of the ship obtained by (11)
- c mode factor defined by $\Delta_1/\int_0^L w_1\eta^2 dx$, where w_1 is distributed load per unit length
- Δ_1 displacement of ship including virtual added weight of water
- π/δ magnification factor of the two node vertical vibration of the ship

The distribution of the exciting force is notable where the distributed force is not a steady vibratory force but a progressive force, as seen in the integrand of equation (12), and the distribution will concentrate near the bow according to the ship side wave distortion. Since the wave height used in the calculation is the one related to the ship motion, no special consideration is necessary to be paid here to the pitching motion, as mentioned in the previous paper.

The estimation of the stress response amidship induced by the bow acceleration is obtained from the method presented in Appendix of authors previous paper[1].

4. Numerical Examples

The springing forces and the responses of a tanker of $230_M \times 34.8_M \times 20.0_M$ with $V=8.0\ _M/s$ in ballast condition are calculated when she is going in head sea, encountering various wave length and wave pattern. The measured envelopes of ship side wave height h_s/h of a self-propelled model tanker were used as an approach. The virtual mass coefficient JC_V of several sections of the hull of a tanker obtained in the author's previous paper are applied correcting the empirical factor according to the method shown in Appendix A2. The buoyant force calculation is shown in Appendix A3. The three types of different wave pattern obtained from the bow pressure measurements on board 76,000 D. W. T. tanker[5] are used in the present numerical calculation. (see also Table AI in Appendix A2)

Figure 4(a), (b) and (c) show three examples of the caculated results of distributions of progressive force exciting hull springing along ship length. It is notable that, when $n=1$, the buoyant force along ship length surpasses, as seen in Fig, 4 (a). The virtual mass force is concentrated almost to the entrance of the hull, according to the consideration of ship side wave distortion except lower values of n, as seen in Fig. 4 (b).

As one of the results of the present investigation, the range of distribution of the wave-induced force exciting sprining may be considered merely as that of the length of the entrance of the hull of a tanker in the higher values of n. Fig. 4 (c) shows the exciting force in the case of pitching resonance, and it is

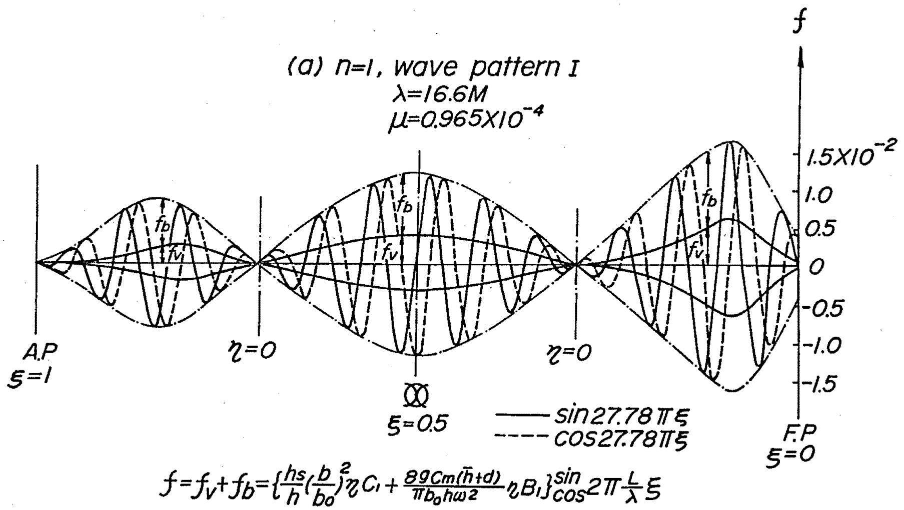

Fig. 4 (a), (b), (c), Progressive exciting force distributed along ship length

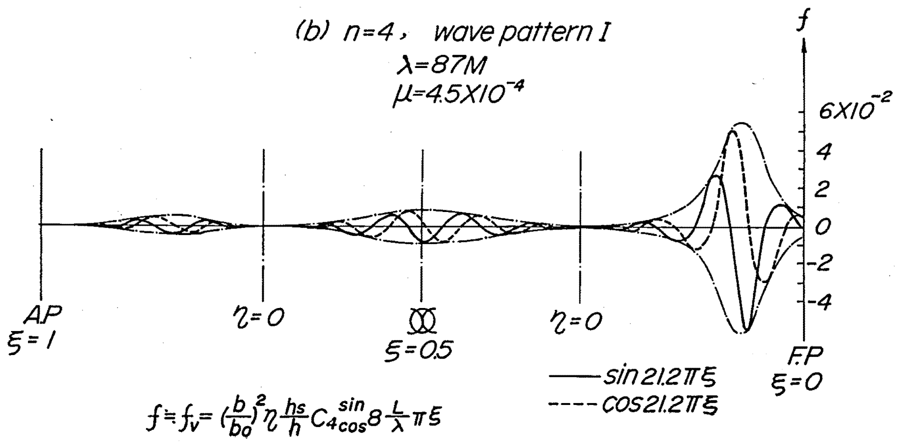

Fig. 4 (b)

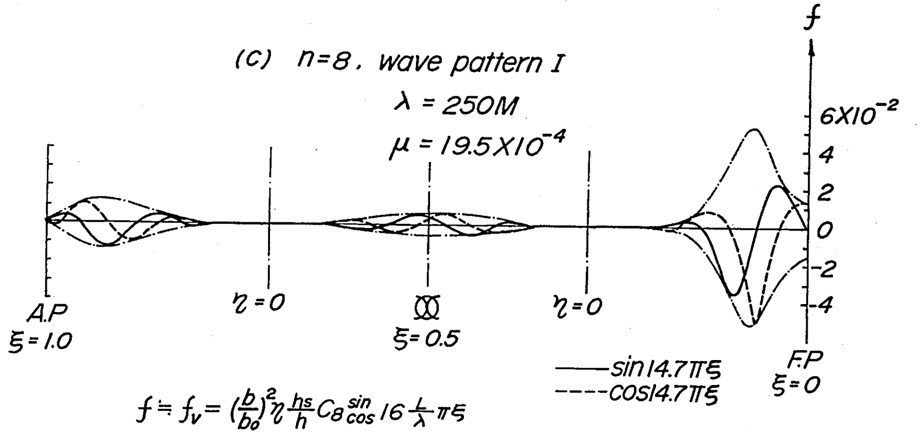

Fig. 4 (c)

of interest that a little quantity of the force distribution appears near to the stern.

With regards to the buoyant force, the buoyant force is estimated about 75 % of total force when n takes unity, 43 % for $n=2$ and 18 % for $n=3$. It is however, so small as negligible over $n=4$ in the wave pattern I. The force amplitudes have considerable effect to the wave pattern when n becomes a high value.

Figure 5 shows the calculated results of force and response versus wave pattern presented by the third harmonic component a_3 with the same numerical assumptions of the mode factor $c=10$, and magnification factor of the hull vibration $\pi/\delta=80$, as that assumed in previous paper[1]. It is interesting to find that there are some irregularity of force and response in each wave pattern and n-value. In general cases, the force and response almost vanish more over $n=9$ in all wave patterns in the present calculation. This phenomena will be confirmed by springing experiment by using a similar ship model as shown in Appendix A1.

In the present calculation, the height of sea wave, h, is assumed to be equal to 1/20 in all wave length, and h_s/h values are taken from the model experiment results. Since the wave height ratio h/λ in experiments is about 1/30 to 1/25, so some correction of h_s/h for wave height ratio should be taken into account in the present estimation of exciting force. It seems that results of the force and response of springing of a tanker obtained from the present estima tion show a little high value as seen in Figure 5, the result of the present estimation will be reduced by the above mentioned correction of h_s/h for h/λ.

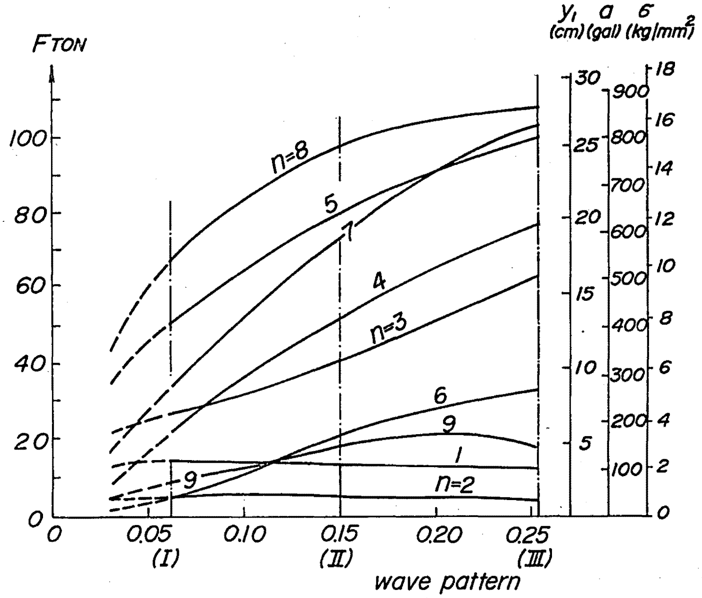

Fig. 5 Exciting force and response of springing of 76,000 D. W. T. tanker with various wave pattern. F_n and a are exciting force and acceleration at the fore perpendiculer respectively and σ is stress induced amidship of the hull

5. Relation between Bending Moment of Hull due to Springing and Wave Bending Moment

The exciting force of springing of a ship in the case $n \geqq 4$ is considered to be proportional to B^2L, as seen in equation (11), where B and L are breadth and length of ship respectively, provided that only the hull structure is considered. On the other hand, the wave bending moment divided length L is approximately assumed to be proportional to the displacement of the ship that $L \cdot B \cdot d$ in the same hull, where d is the draught. Since the draught is assumed to be proportional to the depth D, the ratio of two types of bending moment of the same ship hull will become,

$$\frac{\text{Bending moment due to springing}}{\text{Wave bending moment}} = k\frac{B}{D} , \qquad (14)$$

where, k is constant.

It is expected that the possibility of occurrence of severe springing is judged by B/D-value in the ship form of a tanker or a bulk carrier and that the more the B/D-value increases, the severer springing occurs.

6. Conclusions

Since the relative ship side wave height is two to three times higher at the bow and the half to quater lower at the stern than that of sea wave in the hull form of a tanker in the present model experiments, the effect of ship side wave upon the exciting force and response of the hull springing is certainly obtained in the distribution of the progressive force along ship length, which appear only in the range of the entrance of the hull, in the higher values of n. There is such an effect of wave pattern on the wave-induced force that the more the higher harmonics of the wave pattern increases, the more the virtual mass force increases, except for the lower values of n. As a method of the evaluations of the ratio of bending moment produced by springing to the wave bending moment, the determination of B/D-value of a tanker or a bulk carrier is available for initial design of ship hull as a criterion of springing.

The author believes it necessary to further studies on the excitation of the hull springing on the different hull forms from a tanker taking into account the correction of ship side wave with respect to wave height in sea way.

The author is much indebted to Mr. Y. Sakurada, Mr. H. Komatsu and Miss Y. Uchino of the institute for their assistance in the experiments and numerical calculations.

References

1) Kumai, T., Wave-Induced Force Exciting Hull Vibration and its Response, Trans. West-Japan Soc. N. A. No. 44, 1972, p. 33.
2) Grim, O., Durch Wellen an einem Schiffskörper erregte Kräfte, Symposium on the behavier of ship in a sea way, Wageningen, Chap. 14, 1957, p. 232.
3) Watanabe, Y., On a Cause of Whipping, Rep. of Western Ship Struct. Comm. Japan, No. 66, 1968.
4) Kumai, T., A Method for Evaluating the Three-Dimensional Reduction Factor of the Virtual Mass in the Vertical Vibration of Ships. Japan Shipbld. and Marine Eng. Vol. 1, No. 3, 1966, p. 15.
5) Kumai, T. and Tasai, F., On the Wave Exciting Force and Response of Whipping of Ships, Europ. Shipbld. No. 4, 1970, p. 42.

(Received November 30, 1972)

Appendix

A 1. Model Experiments for Confirming the Hull Springing as a Selective Resonance

An ordinary wooden ship model has natural frequency of vertical vibration much higher than the encounter frequency to wave in the experimental tank. The natural frequency of the model ship for observing springing should be determined by the following similitude,

$$f_m = \sqrt{\frac{L_s}{L_m}} \cdot f_s \ ,$$

where, f_m, f_s natural frequencies of vertical vibration of model ship and actual ship respectively

L_m, L_s length of model ship and actual ship respectively

For reducing the natural frequency, f_m, of vertical vibration of the wooden model tanker of length 2.5 metre, the model was cut out ten blocks at the main station, and set up again by the aluminium flat strips of cross section 60 mm $\times$ 4 mm with tapered both ends close to the neutral axis of section of insides of the model block with some clearance of each block, as shown in Figure A1.

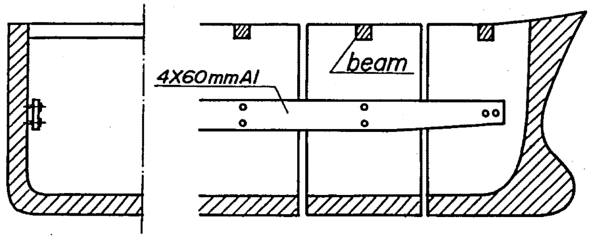

Fig. A 1 Model used for springing experiments

The self-propeled model tests were carried out using the above mentioned model, at different speed of a ship and in various wave length measuring the strain of flat strip at the midship produced by springing. The measured results are shown in Figures A2 and A3. The phenomena of the springing will be clearly observed as the selective resonance with periodic wave force, and it is qualitatively confirmed by the present model experiments. The measurements of strain were carried out for $n=4$ to $n=10$. The resonance over $n=11$ vanishes. It seems that the maximum amplitude of springing will occur nearer to the period of the resonance of pitching motion of the ship in the present experiments.

A 2. Correction of Coefficients of Power Series for Representing the Three-Dimensional Virtual Added Mass of the Hull Section with Varying Draught

The natural frequencies of cylindrical models of typical cross sections with the same length of the ship model are measured in air and in water with various draught up to the $d+\bar{h}$, and JC_V are obtained from measured natural frequencies by the following equation,

$$JC_V = \frac{2m_1}{\rho\pi b^2}\left(\frac{f_a^2}{f_w^2} - 1\right) , \tag{A 1}$$

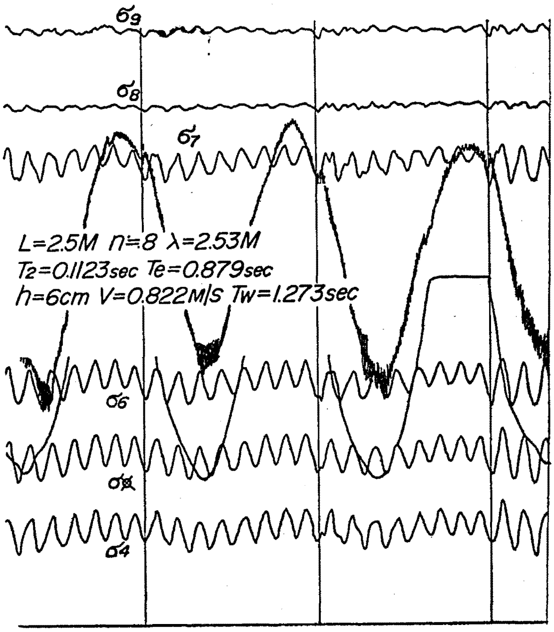

Fig. A 2 An example of osscillogram of model ship, σ_s show strain of bar at each station

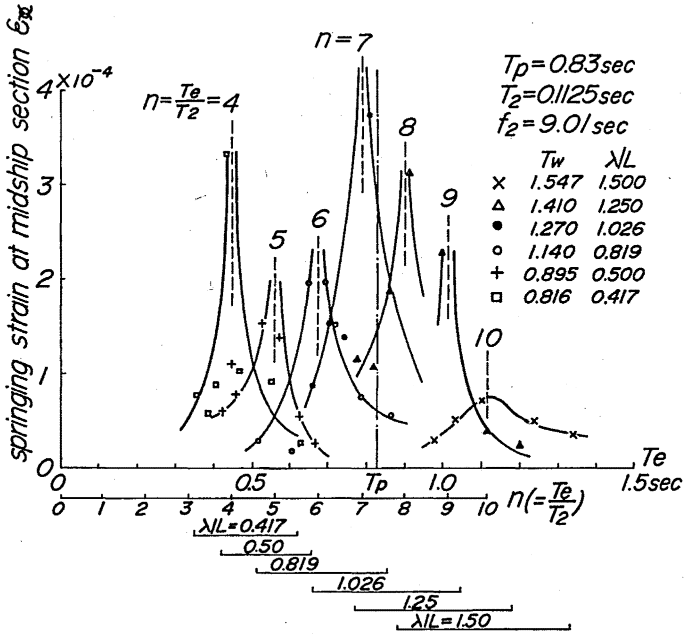

Fig. A 3 Result of experiments for confirming hull springing as selective resonance where, m_1 mass per unit length of the cylindrical model

b a half breadth of model at the water line $d+\overline{h}$ of given section

f_a, f_w two node natural frequencies of the model measured in air and in water respectively

The calculated JC_V in each section is plotted for various draughts from zero to $d+\overline{h}$ of z-axis, as shown in Figure A4 (a). Since the wave is progressive and changes its height along ship length, the draught of each section will be assumed up to the crest of ship side wave from deformed water line measured when ship is going in smooth water, as seen by the chain line in Figure A4 (b). If we assume the wave profile is sinusoidal, for the sake of simplicity, the envelopes of the wave crest and the wave trough are approximately drawn $\pm h_s/2$ from the water line, as shown in Figure A4 (b). Now, we consider the new abscissa Z as follows,

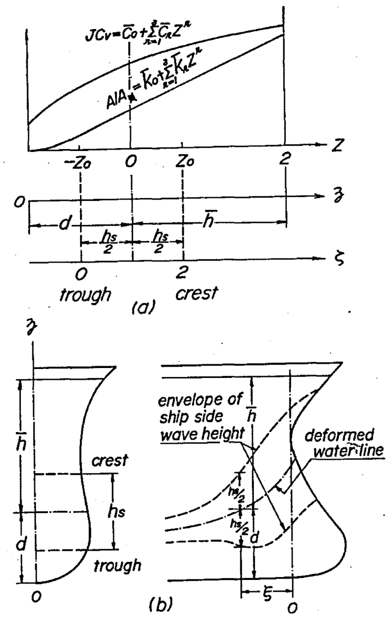

Fig. A 4 (a), (b), Co-ordinate of z, Z and ζ

$$Z=\frac{2(z-d)}{\overline{h}}, \tag{A 2}$$

where, $\overline{h}$ assumed maximum wave height tested

The curve of JC_V may be then expressed by power series with respect to Z, that

$$JC_V=\overline{c}_0+\sum_{r=1}^{3}\overline{c}_r Z^r \tag{A 3}$$

If the ship side wave height is obtained from the model tests, we will get Z_0 as follows by putting $z-d=h_s/2$,

$$Z_0=\frac{h_s}{h} \tag{A 4}$$

The abscissa Z is transformed again to abscissa ζ, in which the maximum value is $\zeta=2$ at the wave crest and $\zeta=0$ at the wave trough. The expression of the relation between the virtual added mass and ζ is then written by

$$JC_V=\bar{c}_0+\sum_{r=1}^{3}\bar{c}_r Z^r(\zeta-1)^r$$

$$=c_0+\sum_{r=1}^{3}c_r\zeta^r \ ,$$

JC_V produced by wave is written as follows,

$$\delta JC_V=JC_V(\zeta)-JC_V(0)=\sum_{r=1}^{3}c_r\zeta^r \ , \tag{A 5}$$

where,

$$c_1=\bar{c}_1Z_0-2\bar{c}_2Z_0^2+3\bar{c}_3Z_0^3$$
$$c_2=\bar{c}_2Z_0^2-3\bar{c}_3Z_0^3$$
$$c_3=\bar{c}_3Z_0^3$$
$$\zeta=a_0+\sum_{m=1}^{3}a_m\cos m\left(\omega t-\frac{2\pi L}{\lambda}\xi\right)$$

The numerical values of a_0, a_m and $\bar{c}_0$, $\bar{c}_r$ are shown in Table AI and Table AII respectively. Substitute ζ into (A5), we get

$$\delta JC_V=\sum_{n=1}^{3}C_n\cos(n\omega t-\psi_n) \ , \tag{A 6}$$

$$\psi_n=\frac{2n\pi L}{\lambda}\xi \ . \tag{A 7}$$

Table A I Components of three types of wave patterns obtained from measurements of bow pressure on board 76,000 D. W. T. tanker

wave pattern	a_0	a_1	a_2	a_3
I	0. 8125	0. 9375	0. 1875	0. 0625
II	0. 8060	0. 8500	0. 1940	0. 1500
III	0. 8000	0. 7470	0. 2000	0. 2530

The cosine components C_n and phase lag ψ_n are calculated as follows;

$$C_1=\{a_0a_1+\frac{1}{2}a_2(a_1+a_3)\}c_1+\{a_0^2a_1+a_0a_2(a_1+5a_3)-\frac{1}{4}a_1^3-\frac{1}{4}a_1^2(a_3+2a_2)+$$

$$\frac{1}{4}a_2^2a_3+\frac{1}{2}a_1(a_1^2+a_2^2+a_3^2)\}c_2+[a_0^3\{a_1+\frac{1}{2}a_2(a_1+a_3)+a_0^2a_2(a_1+a_3)$$

$$+\frac{1}{4}a_0\{(a_1^2+a_2^2+a_3^2)(2a_1+a_1a_2+a_2a_3)+3(a_1^2+a_2^2)+4a_1(a_2^2+a_3^2)$$

$$+2a_1^3\}+\frac{a_1a_2}{8}(3a_1^2+2a_2^2+4a_3^2-a_2^2+2a_1-a_1a_3)+\frac{a_2a_3}{8}\{3(a_2+a_3^2)-2$$

$$(a_3+a_2^2))\}]c_3$$

$$\psi_1=\frac{2\pi L}{\lambda}\xi$$

$$C_2=\{4a_0a_2+a_1(a_1+2a_3)\}c_1+2\{a_0a_1(a_1+2a_3)+a_2(2a_0^2+a_1a_3+a_1^2+\frac{1}{2}a_2^2+a_3^2)\}$$

$$c_2+2[a_0^3(\frac{1}{2}a_1^2+a_1a_3+2a_2)+a_0^2(a_1^2+2a_1a_3)+a_0\{(a_1^2+a_2^2+a_3^2(a_2+\frac{1}{4}$$

$$a_1^2+\frac{1}{2}a_1a_3)+5a_1a_2a_3+\frac{3}{2}a_2^3+2a_2(a_1^2+a_3^2)\}+\frac{a_1a_2}{4}(2a_1a_2+7a_2a_3)+\frac{a_1a_3}{8}$$

$$(3a_1-8a_3^2+4a_1a_3+3a_3^2-a_1^2)+\frac{3}{8}a_2^2a_3^2]c_3$$

$$\psi_2=\frac{4\pi L}{\lambda}\xi$$

$$C_3=\frac{9}{2}\{2a_0a_3+a_1a_2\}c_1+3\ \{3a_0(a_0a_3+a_1a_2)+\frac{a_1}{4}(3a_2^2-2a_1^2)+\frac{1}{2}a_3(a_1^2+a_2^2+a_3^2)\}\ c_2$$

$$+3\Big\{\frac{3}{2}a_0^3(2a_3+a_1a_2)+3a_0^2a_1a_2+\frac{3}{4}a_0(a_1^2+a_2^2+a_3^2)(2a_3+a_1a_2)+\frac{a_0a_1}{4}(3a_1^2$$

$$+11a_2^2+12a_1a_3)+\frac{a_0a_2}{4}(12a_2^2-7a_3^2)+\frac{a_1a_2}{8}(a_2+8a_2^2+21a_3^2)+\frac{a_1^2a_2}{8}\ (2+$$

$$a_1+9a_3)+\frac{3}{8}a_2^2a_3(2a_2-1)\Big\}\ c_3$$

$$\psi_3=\frac{6\pi L}{\lambda}\xi$$

$$C_4=4(2a_1a_3+a_2^2)c_1+4\{2a_0(2a_1a_3+a_2^2)+\frac{1}{2}a_1^2(a_2+a_3)+a_2a_3(a_1+a_3)\}c_2+4\ \{a_0^3$$

$$(2a_1a_3+\frac{1}{2}a_2^2)+2a_0^2(2a_1a_3+a_2^2)+a_0a_1a_2(3a_1+6a_3+a_2a_3+\frac{1}{4}a_1a_2)+a_0a_2a_3$$

$$(3a_3+\frac{1}{4}a_2a_3)+a_0a_1a_3(a_1^2+a_3^2)+\frac{1}{4}a_0a_2^4+\frac{a_1}{8}(a_1^2+a_3^2+3a_1a_3)+a_1a_2^2(a_1$$

$$+a_3)+\frac{3}{8}a_1a_3^2(a_3-a_1)+a_3(a_2^2a_3+\frac{1}{8}a_1^3)\}c_3$$

$$\psi_4 = \frac{8\pi L}{\lambda}\xi$$

$$C_5 = \frac{25}{2}a_2a_3c_1 + \frac{25}{4}\{4a_0a_2a_3 + a_1(a_2^2 + a_3^2 + a_1a_3)\}c_2 + \frac{5}{8}[2a_0a_1(15a_2^2 + 17a_3^2 9a_1a_3)$$
$$+ a_2a_3\{60a_0^2 + 2a_3 + 3a_2 + 10(a_0+2)a_1^2 + 9a_1a_3 + 2(5a_0+1)a_2^2 + (10a_0+3)a_3^2\}$$
$$+ a_1a_2(2a_1 - a_2 + 3a_1^2 + 6a_2^2)]c_3$$

$$\psi_5 = \frac{10\pi L}{\lambda}\xi$$

$$C_6 = 9a_3^2c_1 + 3\{6a_3(a_0a_3 + a_1a_2)a_2^3\}c_2 + \frac{9}{4}[4a_0a_2\,(6a_1a_3 + a_2^2) + a_2^2\,(4a_1a_3 + 4a_3^2 +$$
$$3a_1^2) + a_1^2a_3(4a_3 + a_1 + 1) + 4a_3^2\{3a_0^2 + \frac{1}{2}a_0(a_1^2 + a_2^2 + a_3^2)\}]c_3$$

$$\psi_6 = \frac{12\pi L}{\lambda}\xi$$

$$C_7 = \frac{49}{4}a_3(a_1a_3 + a_2^2)c_2 + \frac{7}{8}\{42a_0a_3(a_2^2 + a_1a_3) + a_2a_3(9a_1a_3 + 21a_1^2 + 7a_3) + a_1a_2^2$$
$$(6a_2+1)\}c_3$$

$$\psi_7 = \frac{14\pi L}{\lambda}\xi$$

$$C_8 = 16a_2a_3^2c_2 + \{3a_2a_3(16a_0a_3 + 5a_1a_2) + 3a_1a_3^2(4a_1 + 3a_3) + 2a_2^3 - a_1a_3^2\}c_3$$

$$\psi_8 = \frac{16\pi L}{\lambda}\xi$$

$$C_9 = \frac{27}{4}a_3^3c_2 + \frac{27}{8}\{a_3^2(6a_0a_3 + 5a_1a_2) + a_2^2a_3(2a_2+1)\}c_3$$

$$\psi_9 = \frac{18\pi L}{\lambda}\xi$$

$$C_{10} = a_3^2\left\{\frac{5}{4}a_1 + \frac{45}{4}a_2^2 + a_1a_3\right\}c_3$$

$$\psi_{10} = \frac{20\pi L}{\lambda}\xi$$

$$C_{11} = \frac{11}{4}a_3^2\{a_2 + \frac{9}{2}a_2a_3\}c_3$$

$$\psi_{11} = \frac{22\pi L}{\lambda}\xi$$

$$C_{12} = \frac{9}{2}a_3^3c_3$$

$$\psi_{12} = \frac{24\pi L}{\lambda}\xi$$

Table A II Coefficients $\bar{c}_0$ and $\bar{c}_r$ obtaind from experiments of cylindrical models of various hull sections

ξ	$\bar{c}_0$	$\bar{c}_1$	$\bar{c}_2$	$\bar{c}_3$
0	0.840	0.192	-0.115	0.0333
0.05	0.530	0.230	-0.125	0.0250
0.10	0.655	0.200	-0.135	0.0550
0.15	0.760	0.115	-0.142	0.0950
0.2	0.780	0.085	-0.148	0.0975
0.3	"	"	"	"
0.4	"	"	"	"
0.5	"	"	"	"
0.6	"	"	"	"
0.7	"	"	"	"
0.8	0.578	0.152	-0.130	0.050
0.85	0.370	0.212	-0.095	0.023
0.90	0.140	0.200	0.010	-0.010
0.95	0.020	0.107	0.080	-0.007
1.0	0	0	0	0

A 3. Expression of Buoyant Force by Cosine Series

The areas of typical sections of the hull are measured from body plan up to the water line $\bar{h}+d$, and curves of the area ratio are obtained, as shown in Figure A4 (a) with the same abscissa Z, as used in Appendix A2. The transformation of the abscissa Z to ζ can be carried out by the similar method, as shown in Appendix A2. The expression of the area function is written by,

$$f(Z)=\bar{k}_0+\sum_{r=1}^{3}\bar{k}_r Z^r \tag{A 8}$$

and

$$f(\zeta)=k_0+\sum_{r=1}^{3}k_r\zeta^r \tag{A 9}$$

It is to be noted that the buoyant force function is corresponding to the increased sectional area produced by wave height h_s, which will be written as follows,

$$f(\zeta)-f(o)=\sum_{r=1}^{3}k_r\zeta^r\ , \tag{A 10}$$

where,

$$k_1=\bar{k}_1Z_0-2\bar{k}_2Z_0^2+3\bar{k}_3Z_0^3$$

$$k_2=\bar{k}_2Z_0^2-3\bar{k}_3Z_0^3$$

$$k_3=\bar{k}_3Z_0^3$$

The coefficients $\bar{k}_r$ of the power series in the hull form of tanker are shown Table AIII. The right hand side of (A10) is represented by cosine series, that

$$\sum_{r=1}^{3}k_r\zeta^r=\sum_{n=1}^{3}B_n\cos(n\omega t-\psi_n) \tag{A 11}$$

The n-th order components B_n are computed as follows. The phase lags are taken as the same value as that of Appendix A2.

Table A III Coefficient $\bar{k}_0$ and $\bar{k}_r$

ξ	$\bar{k}_0$	$\bar{k}_1$	$\bar{k}_2$	$\bar{k}_3$
0	0.063	0.050	-0.0130	-0.00016
0.05	0.140	0.175	0.0275	-0.00733
0.1	0.225	0.260	0.0320	-0.00733
0.15	0.280	0.300	0.0225	-0.00660
0.2	0.330	0.325	0.0160	-0.00610
0.3	0.405	0.358	0.0150	-0.00320
0.4	//	//	//	//
0.5	//	//	//	//
0.6	//	//	//	//
0.7	0.415	0.282	0.0045	-0.00150
0.8	0.355	0.238	0.0072	-0.00025
0.85	0.284	0,208	0.0210	-0.00570
0.9	0.190	0.120	0.0090	0.01030
0.95	0.073	0.060	0.0017	0.01130
1.0	0	0	0	0

$$B_1 = a_1k_1 + (2a_0a_1 + a_1a_2 + a_2a_3)k_2 + \left\{\frac{3}{4}\left(\frac{4}{3}a_1a_0^2 + a_1^3 + a_1^2a_3 + 2a_1a_2^2 + 2a_1a_3^2\right) + (2a_0^2a_1 + 3a_0a_1a_2 + 3a_0a_2a_3 + \frac{1}{2}a_2^2a_3)\right\}k_3$$

$$B_2 = a_2k_1 + \left(\frac{1}{2}a_1^2 + 2a_0a_2 + a_1a_3\right)k_2 + \frac{3}{2}(2a_0^2a_2 + a_0a_1^2 + a_1^2a_2 + \frac{1}{2}a_2^3 + a_2a_3^2 + 2a_0a_1a_3 + \frac{1}{3}a_1a_2a_3)k_3$$

$$B_3 = a_3k_1 + (2a_0a_3 + a_1a_2)k_2 + \frac{3}{4}(4a_0^2a_3 + 2a_1^2a_3 + \frac{1}{3}a_1^3 + 2a_2^2a_3 + a_1a_2^2 + a_3^3 + 4a_0a_1a_2)k_3$$

$$B_4 = \left(\frac{1}{2}a_2^2 + a_1a_3\right)k_2 + \frac{3}{4}(a_1^2a_2 + 2a_0a_2^2 + \frac{1}{3}a_2^3 + a_2a_3^2 + 4a_0a_1a_3 + 2a_1a_2a_3)k_3$$

$$B_5 = a_2a_3k_2 + \frac{3}{4}(a_1^2a_3 + a_2^2a_1 + a_1a_3^2 + 4a_0a_2a_3)k_3$$

$$B_6 = \frac{1}{2}a_3^2k_2 + \frac{3}{2}(a_0a_3^2 + a_1a_2a_3)k_3 \qquad B_8 = \frac{3}{4}a_2a_3^2k_3$$

$$B_7 = \left(\frac{3}{4}a_1a_3^2 + \frac{1}{2}a_2^2a_3\right)k_3 \qquad B_9 = \frac{1}{4}a_3^3k_3$$

A 4. Analytical Integral of Progressive Force

Since the numerical integrals of equation (12) are so much tedious to calculate, the analytical integral is examined as an approach provided that the force envelope is assumed to be of the integrable function. The integrand of equation (12) except low value of n will be approximately replaced integrable function as follows,

$$\left(\frac{b}{b_0}\right)^2 \frac{h_s}{h} \eta C_n \frac{\sin}{\cos} \beta\pi\xi \equiv C'_n f(\xi) \frac{\sin}{\cos} \beta\pi\xi \ , \qquad 0 \leqq \xi \leqq \frac{1}{4} \ , \tag{A 12}$$

where, C'_n maximum value of force envelope of n-th order distributed function

$f(\xi)$ integrable function normalized at maxmum point of envelope

$\beta = \frac{2nL}{\lambda}$

Now, we put $f(\xi)$ a parabola of the third order, that is approximately similar curve to the force envelope, that

$$f(\xi) = a\xi\left(\frac{1}{4} - \xi\right)^2 \ , \qquad 0 \leqq \xi \leqq \frac{1}{4} \tag{A 13}$$

where, $a=432$, provided that the curve is normalized at $\xi=0.0833$

Integrating right hand side of (A12), which cons'st of two equations with respect to ξ from 0 to 1/4 by using (A13), the resultant μ_n is written by

$$\mu_n \doteqdot C'_n \frac{27}{(\beta\pi)^2} \sqrt{1+5\left(\frac{8}{\beta\pi}\right)^2 + \frac{16}{\beta\pi}\left(\sin\frac{\beta\pi}{4} + \frac{16}{\beta\pi}\cos\frac{\beta\pi}{4}\right)} \tag{A 14}$$

The exciting force is thus obtained for various n-values, as shown in Table AIV.

Table A IV Exciting forces obtained from analytical and graphycal integrals in wave pattern I

n	F (ton)	
	analytical approach	graphycal
1	9.6	14.5
2	5.8	4.5
3	24.4	27.2
4	15.45	22.0
5	36.5	50.5
6	2.5	5.5
7	20.6	34.5
8	20.0	67.0
9	4.4	8.3

For calculating the exciting force, μ_n-value in equation (12) will be conveniently estimated by (A14) as practical use.